

Surface complexation modeling of zinc sorption onto ferrihydrite

James A. Dyer,^{a,b,*} Paras Trivedi,^c Noel C. Scrivner,^b and Donald L. Sparks^a

^a Department of Plant and Soil Sciences, University of Delaware, Newark, DE 19717, USA

^b DuPont Engineering Technology, Brandywine Building, Wilmington, DE 19898, USA

^c Department of Civil and Environmental Engineering, University of Alaska Fairbanks, Fairbanks, AK 99775, USA

Received 14 March 2003; accepted 6 June 2003

Abstract

A previous study involving lead(II) [Pb(II)] sorption onto ferrihydrite over a wide range of conditions highlighted the advantages of combining molecular- and macroscopic-scale investigations with surface complexation modeling to predict Pb(II) speciation and partitioning in aqueous systems. In this work, an extensive collection of new macroscopic and spectroscopic data was used to assess the ability of the modified triple-layer model (TLM) to predict single-solute zinc(II) [Zn(II)] sorption onto 2-line ferrihydrite in NaNO₃ solutions as a function of pH, ionic strength, and concentration. Regression of constant-pH isotherm data, together with potentiometric titration and pH edge data, was a much more rigorous test of the modified TLM than fitting pH edge data alone. When coupled with valuable input from spectroscopic analyses, good fits of the isotherm data were obtained with a one-species, one-Zn-sorption-site model using the bidentate-mononuclear surface complex, ($\equiv\text{FeO}$)₂Zn; however, surprisingly, both the density of Zn(II) sorption sites and the value of the best-fit equilibrium “constant” for the bidentate-mononuclear complex had to be adjusted with pH to adequately fit the isotherm data. Although spectroscopy provided some evidence for multinuclear surface complex formation at surface loadings approaching site saturation at pH ≥ 6.5 , the assumption of a bidentate-mononuclear surface complex provided acceptable fits of the sorption data over the entire range of conditions studied. Regressing edge data in the absence of isotherm and spectroscopic data resulted in a fair number of surface-species/site-type combinations that provided acceptable fits of the edge data, but unacceptable fits of the isotherm data. A linear relationship between $\log K_{(\equiv\text{FeO})_2\text{Zn}}$ and pH was found, given by $\log K_{(\equiv\text{FeO})_2\text{Zn at 1 g/l}} = 2.058 (\text{pH}) - 6.131$. In addition, a surface activity coefficient term was introduced to the model to reduce the ionic strength dependence of sorption. The results of this research and previous work with Pb(II) indicate that the existing thermodynamic framework for the modified TLM is able to reproduce the metal sorption data only over a limited range of conditions. For this reason, much work still needs to be done in fine-tuning the thermodynamic framework and databases for the TLM.

© 2003 Elsevier Inc. All rights reserved.

Keywords: Zinc; Metals; Sorption; Surface complexation modeling; Ferrihydrite; Hydrous ferric oxide; Ferric hydroxide; Triple layer model

1. Introduction

Until the recent development and application of X-ray absorption spectroscopy to delineate trace-metal speciation on mineral oxide and hydroxide, clay mineral, and soil surfaces, equilibrium constants for trace-metal surface complexation reactions in the open literature were largely determined by fitting a small number of single-solute pH sorption edges covering a narrow range of environmental conditions. In most cases, however, this restricts one’s ability to reliably simulate multisolute sorption reactions in complex industrial and environmental systems using any of the surface com-

plexation models (SCMs) found in commercial and public domain geochemical modeling codes.

Over the past several decades, many researchers have studied the sorption of metal cations and anions onto amorphous iron oxides and hydroxides. For example, single-solute sorption data for hydrous ferric oxide (HFO) from before 1990 were critically assessed and modeled by Dzombak and Morel [1] using the Generalized Two-Layer Model (GTLM); the result was a set of best-fit intrinsic equilibrium constants (K^{int}) for trace metal cations and anions. A limitation of this study, however, was that only a small fraction of the selected data sets for each metal consisted of constant-pH isotherms. This means that, if the pH sorption edges and isotherms did not cover a broad range of conditions, then the best-fit K^{int} values would likely have limited applicability. In contrast, a much better test of a SCM is to calibrate

* Corresponding author.

E-mail address: james.a.dyer@usa.dupont.com (J.A. Dyer).

it against constant-pH isotherm data covering more than five orders of magnitude in metal concentration at three or more pH values, in addition to pH sorption edge data collected at several ionic strengths.

Zinc(II) [Zn(II)] is a common constituent found in contaminated soils, sediments, and wastewater and groundwater streams. Unlike for lead(II) [Pb(II)], a reasonable blend of edge and isotherm data was found in the peer-reviewed literature for Zn(II) sorption onto various forms of HFO [2]. Many of the studies report pH edge data only [3–10]; however, a fair number of studies present both isotherm and edge data [11–17]. Benjamin [12] published a pH 6.4 isotherm spanning three orders of magnitude in Zn(II) concentration, while Kinniburgh and Jackson's [14] isotherm data cover four log units in Zn(II) concentration at pH 5.5 and pH 6.5. Harvey and Linton [15] provide isotherms at pH values of 6.25, 6.5, 6.75, 7.0, and 7.25 covering 3–3.5 orders of magnitude in Zn(II) concentration. Trivedi and Axe [17] present isotherms at pH 6, pH 7, and pH 8 that cover 3–4 log units in Zn(II) concentration. The three remaining isotherm data sets [11,13,16] span only 1–2 orders of magnitude in Zn(II) concentration. Dzombak and Morel [1] used a blend of Zn(II) edges and isotherms from Leckie et al. [5], Kinniburgh et al. [11], Benjamin [12], Dempsey and Singer [13], and Kinniburgh and Jackson [14] to determine the best-fit surface complexation constants for both Type 1 and Type 2 sites. Surface precipitation reactions were included by Dzombak and Morel [1] in the GTLM only to fit the pH 6.5 isotherm data from Kinniburgh and Jackson [14] at high surface loading. Otherwise, only adsorption reactions were required to fit the data. None of these studies, however, benefited from spectroscopic analyses of the sorbent surface to help confirm surface speciation. In addition, while the collective data set for Zn(II) sorption onto HFO is more impressive than that for Pb(II), the fact remains that the studies were performed by different researchers in different labs under different conditions.

Dyer et al. [2] provide more detailed discussion on the evolution of surface complexation modeling as it pertains to justifying this specific research project. In short, an in-depth literature review highlighted only a few studies where molecular- and macroscopic-scale data had been coupled with surface complexation modeling to predict metal-cation sorption over a wide range of conditions [18–20]. None were found for Zn(II) sorption onto HFO/ferrihydrite. Trivedi et al. [21] present comprehensive single-solute macroscopic and spectroscopic data for Zn(II) sorption onto two-line ferrihydrite, including a review of previous spectroscopic studies aimed at delineating Zn sorption mechanisms on mineral oxides. This paper will emphasize the importance of integrating spectroscopic data on surface speciation with macroscopic isotherm and pH sorption edge data covering a wide range of conditions when calibrating a SCM. In addition, it will point to potential limitations in using an existing SCM, such as the modified triple-layer model (TLM), to determine an optimal set of surface complexation modeling param-

eters for single-solute Zn(II) sorption onto two-line ferrihydrite.

2. Methods

2.1. Potentiometric titration and Zn(II) sorption data

The surface complexation modeling studies in this paper build upon the macroscopic sorption data and X-ray absorption spectroscopy studies detailed in Trivedi et al. [21] for single-solute Zn(II) sorption onto two-line ferrihydrite. All experiments were performed in a N₂ atmosphere at room temperature using a 4-h equilibration time. Trivedi et al. [22] describe the ferrihydrite preparation method and present potentiometric titration data for two-line ferrihydrite in 0.001, 0.01, and 0.1 M NaNO₃ solutions (N₂ atmosphere and room temperature). Analysis of the potentiometric titration data is described in Dyer et al. [2]. Raw tabulated potentiometric titration and Zn(II) sorption data can be found in Dyer [23]. All constant-pH isotherm and pH edge data points were individually equilibrated in their own sample vials. Batch kinetic studies were conducted initially to determine the time required to reach equilibrium with the external surfaces of the ferrihydrite particles using similar boundary conditions to the ones utilized in the constant-pH isotherm studies [21]. Equilibration times from several minutes to 4 d were evaluated. As was previously found for Pb [22], a substantial change in sorption did not occur after 1–2 h. In addition, spectroscopic data at high surface loading gave no indication of potentially slow sorption processes, such as surface precipitation and/or multinuclear complex formation.

2.2. Geochemical modeling software

The OLI Software (OLI Systems Inc., Morris Plains, NJ) was used to perform the simulations in this study. Details on the thermodynamic databank and framework, the equation solvers, the aqueous activity coefficient model, and the SCMs used in the OLI Software are presented in Dyer et al. [2]. More specifically, the ElectroChem solver was used in this study because it performs single-point aqueous equilibrium calculations at steady state [24]. The OLI equilibrium reactions and associated equilibrium constants used in this work are given in Table 1.

2.3. Surface complexation models

The OLI Software offers the user the option of using one of four different SCMs. These include the constant capacitance model (CCM), the GTLM, the TLM, and a nonelectrostatic model (NEM). In this study, the modified TLM was employed, having provided best fits of the Pb(II)/ferrihydrite isotherm and pH edge data presented and analyzed in Trivedi et al. [22] and Dyer et al. [2]. The thermodynamic framework

Table 1
Equilibrium reactions and associated equilibrium constants used in the OLI simulations

Rxn. No.	Equilibrium reaction	log <i>K</i> at 25 °C
1	$\text{H}_2\text{O} = \text{H}^+ + \text{OH}^-$	-13.9938
2	$\text{HNO}_3(\text{aq}) = \text{H}^+ + \text{NO}_3^-$	1.3038
3	$\text{NaNO}_3(\text{aq}) = \text{Na}^+ + \text{NO}_3^-$	1.7344
4	$\text{ZnOH}^+ = \text{Zn}^{2+} + \text{OH}^-$	-5.0799
5	$\text{Zn}(\text{OH})_2(\text{aq}) = \text{ZnOH}^+ + \text{OH}^-$	-5.6054
6	$\text{Zn}(\text{OH})_2(\text{s}) = \text{Zn}^{2+} + 2\text{OH}^-$	-15.7744
7	$\text{Zn}(\text{OH})_3^- = \text{Zn}(\text{OH})_2(\text{aq}) + \text{OH}^-$	-2.9874
8	$\text{Zn}(\text{OH})_4^{2-} = \text{Zn}(\text{OH})_3^- + \text{OH}^-$	-1.1031
9	$\text{Zn}(\text{NO}_3)^+ = \text{Zn}^{2+} + \text{NO}_3^-$	-0.4605
10	$\text{Zn}(\text{NO}_3)_2(\text{aq}) = \text{Zn}^{2+} + 2\text{NO}_3^-$	0.1783
11	$\equiv\text{FeOH}_2^+ = \equiv\text{FeOH} + \text{H}^+$	Table 3
12	$\equiv\text{FeOH} = \equiv\text{FeO}^- + \text{H}^+$	Table 3
13	$\equiv\text{FeOH}_2^+ - \text{NO}_3^- = \equiv\text{FeOH} + \text{H}^+ + \text{NO}_3^-$	Table 3
14	$\equiv\text{FeO}^- - \text{Na}^+ + \text{H}^+ = \equiv\text{FeOH} + \text{Na}^+$	Table 3
15	$(\equiv\text{FeO})_2\text{Zn} + 2\text{H}^+ = 2\equiv\text{FeOH} + \text{Zn}^{2+}$	Table 4

for the modified TLM is described in Sahai and Sverjensky [25].

2.4. Modeling protocol

The methodology used to calibrate the modified TLM in this work is based largely on the modeling protocol outlined in Hayes and Katz [26]. Using the nonlinear regression program in the OLI code, potentiometric titration data for two-line ferrihydrite in NaNO_3 solutions of three different ionic strengths [22] were first used to estimate a best-fit set(s) of metal hydroxide surface parameters for the modified TLM. As found by others [26], different sets of $N_{s, \text{total}}$, C_1 , and $\Delta\text{p}K_a$ parameter values will yield good fits of the surface titration data for inorganic oxides and hydroxides. As detailed in Dyer et al. [2], a three-factor, face-centered-cube (FCC), response-surface experimental design was previously used to determine the values of $N_{s, \text{total}}$, C_1 , and $\Delta\text{p}K_a$ that provide the best fit of the titration data (A_s and C_2 were held constant in the model). The quality of fit of the model to the data was judged based on both visual inspection of a plot of the model-predicted curves against the raw titration data and the value of the regression fit parameter, R_{avg} , which is provided by the OLI nonlinear regression program. The nonlinear regression routine in the OLI code utilizes a Marquardt nonlinear optimization algorithm. In this study, the ratio, R_i , of the calculated to experimental values (or vice versa, such that R_i is always ≥ 1.0) was the objective function minimized. A perfect fit is defined as $R_i = 1.0$; R_i values were equally weighted. R_{avg} was obtained by arithmetically averaging the values of R_i values for each regressed data set. In regressing data points that span 5 to 7 orders of magnitude, such as in constant-pH isotherms, experience over the years has shown that this objective function is more robust than least-squares minimization. Dyer et al. [2] found that the quality of the fit was largely determined by the value C_1 and, to a lesser extent, by $\Delta\text{p}K_a$

and $N_{s, \text{total}}$. On the basis of these results, the values of C_1 , $\Delta\text{p}K_a$, $N_{s, \text{total}}$, A_s , and C_2 were initially fixed at the same values as those used in the Pb(II)/ferrihydrite modeling studies (i.e., 0.725 faraday/m², 5.0, 0.8 mol of sites/mol of Fe, 600 m²/g, and 0.2 faraday/m², respectively) [2]. If $N_{s, \text{total}}$ had to be adjusted to fit the Zn(II) isotherm data, then the potentiometric titration data were re-regressed using the new value for $N_{s, \text{total}}$.

The second step was to narrow the scope of feasible Zn(II) surface complexation reactions at low to moderate surface coverage. This was achieved by assessing the impact of ionic strength on zinc sorption as well as by analyzing the spectroscopy data—the details of which are reported and analyzed in the companion paper [21]. At low to moderate surface loading (0.1–10%) for strongly sorbing metals and at all surface coverages for weakly sorbing metals, previous X-ray absorption fine structure spectroscopy (XAFS) investigations have shown that the dominant sorption mechanism is the formation of a mononuclear surface species [26]. In addition, inner-sphere versus outer-sphere surface complex formation has often been inferred from the impact of ionic strength on sorption [27]. The impact of ionic strength on zinc sorption in this study was evaluated based on pH sorption edges generated at three different ionic strengths.

The presence or absence of multinuclear surface polymers and/or surface precipitates at higher zinc surface loading was determined from the spectroscopy data as well as from the behavior of the equilibrium isotherm curves. The need for multiple site types (i.e., site heterogeneity) and a reasonable starting value for surface site density were also gleaned from the constant-pH isotherm data. Multiple site types may be needed if the slopes of the constant-pH isotherm curves are < 1.0 at low surface loading [28].

Based on the analysis of the isotherm, pH edge, and spectroscopy data outlined above, a suitable set of Zn(II) surface complex species and modified TLM parameters ($N_{s, \text{total}}$, C_1 , C_2 , $\Delta\text{p}K_a$, and A_s) was chosen. Next, best-fit equilibrium constant(s) for single-solute Zn(II) sorption onto ferrihydrite were determined via nonlinear regression of the equilibrium isotherm data, using the assumed set of surface complex species and surface model parameters. The best-fit equilibrium constant(s) were then tested against the pH edge data at several different starting Zn(II) concentrations and ionic strengths. The sensitivity of the model fits to speciation assumptions was also evaluated, although weight was placed on the spectroscopic results and the desire to minimize the number of sites and species types that yielded the best fit of the sorption data. As before, visual inspection of the agreement between the model predictions and raw data and analysis of R_{avg} values for both x [total soluble Zn] and y [mol Zn mol⁻¹ Fe] data from the OLI regression routine were used to judge fit quality. If $N_{s, \text{total}}$ was adjusted to improve the quality of the fit, then the oxide surface parameters were also reoptimized against the potentiometric titration data.

2.5. Uncertainty analysis

Few studies over the years have addressed error propagation through surface complexation models (SCMs). Yet outputs from SCMs, such as trace-metal partition coefficients, are frequently used as input parameters in contaminant fate and transport models to predict trace-metal mobility in aqueous environmental systems. The reality is that SCMs are often fit to limited set(s) of metal sorption data using input parameters with large uncertainties. As a result, it is important to quantify the impact of input-parameter uncertainty on model output-parameter uncertainty as well as to identify the input parameter(s) that have a dominant influence on output uncertainty. The uncertainty analysis methodology utilized in this research [23] was able to (1) quantify the impact of analytical, thermodynamic, and SCM input-parameter uncertainties on the uncertainty in output parameters, such as metal surface loading and soluble metal concentration and (2) identify the input parameters that had the most significant impact on output uncertainty.

Error propagation studies were conducted using ElectroChem's uncertainty analysis module and were based on the constant-pH isotherm and pH sorption edge data for single-solute Zn(II) sorption onto ferrihydrite. The goal was to identify which model input and thermodynamic parameters determined the majority of the uncertainty in the output variables of interest—total Zn in solution (Zn_{aq}) and Zn surface loading (Zn_{sorb}). Table 2 summarizes the uncertainty value assumed for each model input and thermodynamic parameter included in the detailed error propagation studies. Input/thermodynamic uncertainties are reported as either absolute values (standard deviation, σ_i) or relative values (coefficient of variation, COV_i). Uncertainty assumptions for input parameters, such as pH, total Zn(II), and total H_2O , are based on experience and a review of the literature [1]. Uncertainty bounds for the thermodynamic para-

eters were determined by estimating the 95% prediction intervals ($\pm 2\sigma$) for the model fits of the potentiometric titration and Zn(II) isotherm data [23]. Preliminary error propagation studies using ElectroChem found that uncertainties of as much as 150% in the K values (i.e., $COV_i \leq 1.5$) for the aqueous electrolyte solution reactions shown in Table 1 (i.e., reactions 1–10) had a very small impact on the output uncertainties in Zn_{aq} and Zn_{sorb} for all pH values and Zn(II) concentrations considered in this research. Using the uncertainty assumptions in Table 2, ElectroChem's uncertainty analysis module and the Resampling Stats for Windows software (Resampling Stats Inc., Arlington, Virginia) were then utilized to estimate 95% confidence intervals for the constant-pH-isotherm and pH sorption edge model predictions. Details on the Monte Carlo simulation methodology used to generate these confidence intervals can be found in Dyer [23]. ElectroChem's uncertainty analysis module also provides quantitative results on the fraction of the total output uncertainty that is attributable to specific input variables. These results were also analyzed to identify the input variables that had a dominant influence on the output uncertainties in Zn_{aq} and Zn_{sorb} .

3. Results and discussion

3.1. Potentiometric titration data

The point of zero net proton charge (pH_{PZNPC}) for two-line ferrihydrite was determined to be 7.91, as reported previously [2,22]. This falls within the range of point of zero charge values reported by others [1]. Detailed results for and discussion of the three-factor, FCC, response-surface experimental design, including a comparison of the TLM fits to the experimental data, were previously reported in Dyer et al. [2]. In addition, Dyer et al. [2] discuss titration data and model uncertainties ($\pm 2\sigma$) and their resulting impact on the predicted output uncertainties in Zn_{aq} and Zn_{sorb} . This includes data reproducibility and the effects of equilibration time and ferrihydrite solids concentration on the measured surface charge density. As discussed below, the density of proton-active sites ($N_{s, total}$) was increased from 0.8 mol of sites/mol of Fe (the value used in the Pb(II)/ferrihydrite studies) to 1.2 mol of sites/mol of Fe in order to fit the pH 7.5 Zn(II) isotherm data at maximum loading using a bidentate-mononuclear surface complex. As a result, the 0.001, 0.01, and 0.1 M $NaNO_3$ titration data reported in Dyer et al. [2] were reregressed at this higher site density, yielding the revised TLM parameters in Table 3. The graphical results are essentially identical to those shown in Fig. 1 in Dyer et al. [2].

3.2. Zn(II) sorption isotherms and edges

As discussed above in the modeling protocol, macroscopic and spectroscopic data for the Zn(II)/two-line ferrihy-

Table 2

Input/thermodynamic parameters and corresponding uncertainty assumptions^a

Parameter	Standard deviation (σ_i)	Coefficient of variation (COV_i)
Total Zn(II)		0.02
Total ferrihydrite		0.10
Total H_2O		0.03
Total $NaNO_3$		0.10
pH	0.03 pH units	
$\log K_{NO_3^-}^{int}$	0.36 log units	
$\log K_{Na^+}^{int}$	0.36 log units	
$\log K_{(=FeO)_2Zn}^{int}$	0.12 log units	

^a Refer to Tables 3 and 4 for details on the chemical reactions and mass law expressions corresponding to each of the equilibrium constants given above. Definitions for each of the parameters can be found in Appendix A. Preliminary error propagation studies showed that a $COV_i \leq 1.5$ for the K values of the aqueous electrolyte solution reactions listed in Table 1 (i.e., reactions 1–10) had a very small impact on the output uncertainties in Zn_{aq} and Zn_{sorb} under all conditions evaluated in this research.

Table 3
Best-fit TLM oxide surface parameters for ferrihydrite

Parameter	Value
$N_{s, \text{total}}$ (mol/mol)	1.20
A_s (m ² /g)	600
C_1 (faraday/m ²)	0.60
C_2 (faraday/m ²)	0.20
$\log K_{a1}^{\text{int}^a}$	-5.41
$\log K_{a2}^{\text{int}^b}$	-10.41
$\log K_{\text{NO}_3^-}^{\text{int}^c}$	-7.46
$\log K_{\text{Na}^+}^{\text{int}^d}$	8.48
R_{avg}	1.15

^a $\equiv\text{FeOH}_2^+ \rightleftharpoons \equiv\text{FeOH} + \text{H}^+$, where $K_{a1}^{\text{int}} = a_{\text{H}^+} [\equiv\text{FeOH}] \exp(-F\Psi_0/RT) / [\equiv\text{FeOH}_2^+]$.

^b $\equiv\text{FeOH} \rightleftharpoons \equiv\text{FeO}^- + \text{H}^+$, where $K_{a2}^{\text{int}} = a_{\text{H}^+} [\equiv\text{FeO}^-] \exp(-F\Psi_0/RT) / [\equiv\text{FeOH}]$.

^c $\equiv\text{FeOH}_2^+ - \text{NO}_3^- \rightleftharpoons \equiv\text{FeOH} + \text{H}^+ + \text{NO}_3^-$, where $K_{\text{NO}_3^-}^{\text{int}} = a_{\text{H}^+} a_{\text{NO}_3^-} [\equiv\text{FeOH}] \exp(F(\Psi_\beta - \Psi_0)/RT) / [\equiv\text{FeOH}_2^+ - \text{NO}_3^-]$.

^d $\equiv\text{FeO}^- - \text{Na}^+ + \text{H}^+ \rightleftharpoons \equiv\text{FeOH} + \text{Na}^+$, where $K_{\text{Na}^+}^{\text{int}} = a_{\text{Na}^+} [\equiv\text{FeOH}] \exp(F(\Psi_0 - \Psi_\beta)/RT) / a_{\text{H}^+} [\equiv\text{FeO}^- - \text{Na}^+]$.

drite system [21] played a large role in helping to choose and calibrate the SCM. First, the slope of the low-concentration region of each constant-pH isotherm was about 1.0, which suggested that a one-Zn-sorption-site model might be adequate. Second, only a small ionic strength dependence was observed in the pH edge data (50 μM Zn(II); 1 g l⁻¹ ferrihydrite; 0.001, 0.01, and 0.1 M NaNO₃ background electrolyte solutions), which suggests that Zn(II) predominantly forms inner-sphere complexes. Third, the spectroscopic data analysis indicated that a corner-sharing bidentate-mononuclear inner-sphere surface complex dominated over the pH range 4.5–7.5 as detailed in Trivedi et al. [21]. Spectroscopic data were collected at pH 4.5, 5.5, 6.5, and 7.5 in 0.01 M NaNO₃ solutions at 25 °C. For each pH value, three different surface loadings (~0.001, 0.01, and 0.1 mol Zn/mol Fe) were studied. Only a very small contribution from multinuclear Zn(II) surface complexes was indicated in the XAFS model fits of the second shell near site saturation at pH \geq 6.5. Fourth, it appeared likely that a common set of surface species and/or equilibrium constants would be unable to simulate all the sorption data, because of the significant variation in spacing between the constant-pH isotherm curves. This variable spacing between two adjacent isotherm curves is driven by a change in $d[\text{pZn}_{\text{aq}}]/d[\text{pH}]$ at a constant Zn(II) surface loading and, interestingly, remains essentially unchanged from low to high Zn(II) surface loading. The predominant surface reaction mechanism as determined by XAFS, however, appears to be invariant with pH and surface loading. This suggests that the significant variability in spacing between isotherms cannot simply be accounted for by a change in the bulk reaction mechanism at the surface. Fifth, the maximum Zn(II) surface loading for each of the constant-pH isotherms changes with pH, suggesting that the TLM assumption for

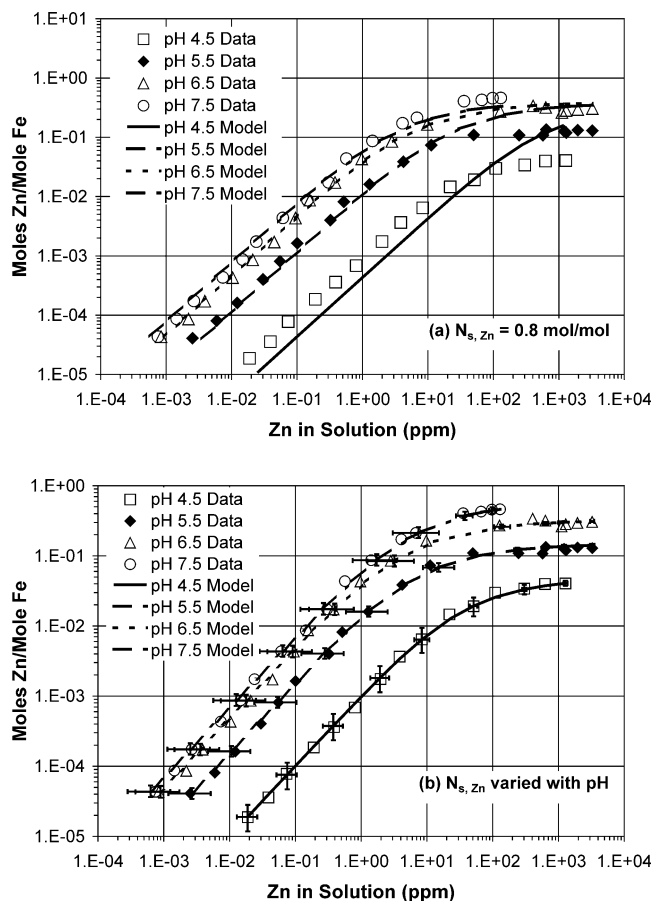


Fig. 1. Optimized triple-layer model fits of pH 4.5, 5.5, 6.5, and 7.5 equilibrium isotherm data for single-solute Zn(II) sorption onto two-line ferrihydrite using the bidentate-mononuclear surface complex, $(\equiv\text{FeO})_2\text{Zn}$. In (a), $N_{s, \text{Zn}}$ was fixed at 0.8 mol of sites/mol of Fe; in (b), $N_{s, \text{Zn}}$ was varied with pH. $\log K_{(\equiv\text{FeO})_2\text{Zn}}$ values as $f(\text{pH})$ are given in Table 4. Ninety-five percent confidence intervals for the model predictions are also shown in (b). Experimental conditions: 0.1 and 1.0 g of ferrihydrite/l in 0.01 M NaNO₃ solution; Zn(II) added as Zn(NO₃)₂; 4-h equilibration time; room temperature; N₂ glovebox.

the site density of available Zn(II) sorption sites needs to be adjusted with pH. As shown in Fig. 1, the maximum sorption capacity of two-line ferrihydrite for Zn(II) is approximately 0.04, 0.13, 0.31, and 0.46 mol of Zn(II)/mol of Fe at pH 4.5, 5.5, 6.5, and 7.5, respectively. As pH increases, the isotherm data clearly appear to plateau at higher surface loadings. This is in contrast to the Pb(II)/ferrihydrite sorption data reported in Dyer et al. [2] where the pH 5.5 and pH 6.5 isotherm data appear to converge at the same maximum sorption capacity of 0.35–0.40 mol of Pb(II)/mol of Fe.

The constant-pH isotherm data are shown in Fig. 1, along with modified TLM fits obtained using the bidentate-mononuclear surface complex $(\equiv\text{FeO})_2\text{Zn}$. In Fig. 1a, the density of Zn-active sites ($N_{s, \text{Zn}}$) was fixed at 0.8 mol of sites/mol of Fe for all pH; in Fig. 1b, the value of $N_{s, \text{Zn}}$ was adjusted with pH to properly capture the variable maximum Zn(II) sorption capacity. In both cases, the nonlinear regression fits of the isotherm data are based on a total density of proton-active sites ($N_{s, \text{total}}$) of 1.2 mol of sites/mol

Table 4

TLM parameters for single-solute Zn(II) sorption onto two-line ferrihydrite (fh)

pH	$N_{s,Zn}^a$ (mol/mol)	$\log K_{(\equiv FeO)_2Zn}$ at 1 g of fh/l ^{b,c}	$R_{avg} (Zn_{aq})^d$	$R_{avg} (\Gamma)^d$
4.5	0.10	3.17	1.02	1.05
5.5	0.30	4.95	1.08	1.05
6.5	0.65	7.15	1.11	1.04
7.5	1.20	9.52	1.11	1.01
4.0	0.075	2.18	–	–
5.0	0.21	4.35	–	–
6.0	0.43	6.01	–	–
7.0	0.90	8.31	–	–
8.0	1.20	10.32	–	–

^a $N_{s, total}$ set at 1.2 mol of proton-active sites/mol of Fe.

^b $(\equiv FeO)_2Zn + 2H^+ = 2\equiv FeOH + Zn^{2+}$, where $K_{(\equiv FeO)_2Zn} = a_{Zn^{2+}} / [a_{\equiv FeOH}^2 / a_{H^+}^2 + \gamma_s [(\equiv FeO)_2Zn]]$. A γ_s correction was used, whereby $\gamma_{(\equiv FeO)_2Zn} = \gamma_{Zn^{2+}}$.

^c For bidentate-mononuclear surface complexes, K^{int} is actually a conditional K that depends on sorbent solids concentration (C_s) regardless. This peculiarity arises with multidentate complexes, because of the definition of the standard state for surface species in molality, rather than mole fraction. It can be shown that $K^{int} = K^{cond} / B$, where $B = N_s$ (sites/m²) $\times A_s$ (m²/g) $\times C_s$ (g/l) / N_A (6.02×10^{23} sites/mol of sites). Hence, $K_2^{cond} / K_1^{cond} = C_{s2} / C_{s1}$ for the bidentate-mononuclear reactions written here as dissociation reactions. The bidentate-mononuclear K values reported in the table are based on 1 g of ferrihydrite/l.

^d R_{avg} reported for regressions of pH 4.5, 5.5, 6.5, and 7.5 isotherm data only. K values for other pH values are approximate based on regression of a few pH edge points only. The intent is to show how K varies with pH.

of Fe. It is evident from Fig. 1b that adjusting $N_{s,Zn}$ results in excellent fits of the Zn(II)/ferrihydrite sorption data over six orders of magnitude in Zn(II) concentration. Equilibrium constants, Zn-active site densities, associated equilibrium re-

actions and mass law expressions, and R_{avg} values for the preferred pH 4.5, 5.5, 6.5 and 7.5 isotherm fits (Fig. 1b) are summarized in Table 4. As noted in Table 4 and explained in more detail below, a surface activity coefficient correction was included in the model fits of the isotherm data to better represent the impact of ionic strength on Zn(II) sorption. Equilibrium constants for the bidentate-mononuclear Zn(II) surface complex are reported as conditional K values (K_i), rather than as intrinsic K values (K_i^{int}), because of the dependence on pH and site density. Regression of the isotherm data using multispecies and/or multi-Zn-sorption-site models (data not given) resulted in inferior fits when compared to the one-Zn-sorption-site bidentate-mononuclear model. Although not supported by spectroscopic data, the species $\equiv FeOZnOH$ provided essentially the same quality of fit as the bidentate-mononuclear surface complex (figure not shown; see Dyer [23]). Mathematically, the mass law expression for $\equiv FeOZnOH$ looks very similar to the mass law expression for $(\equiv FeO)_2Zn$.

Figure 2 emphasizes the very good agreement (i.e., the internal consistency) between the pH sorption edge data and the constant-pH isotherm data. The model-predicted curves for pH 4, 5, 6, 7, and 8 represent fits of the TLM to the pH sorption edge data alone. Oxide surface parameters for the TLM (Table 3) and the assumed surface speciation were the same as those used to regress the pH 4.5, 5.5, 6.5, and 7.5 isotherm data. Conditional equilibrium constants for the bidentate-mononuclear Zn(II) surface complex and estimated values for $N_{s,Zn}$ for each pH value are given in Table 4.

Figure 2 also helps to emphasize the reason that the surface complexation equilibrium constants for Zn sorption are not constant for this comprehensive data set. More specif-

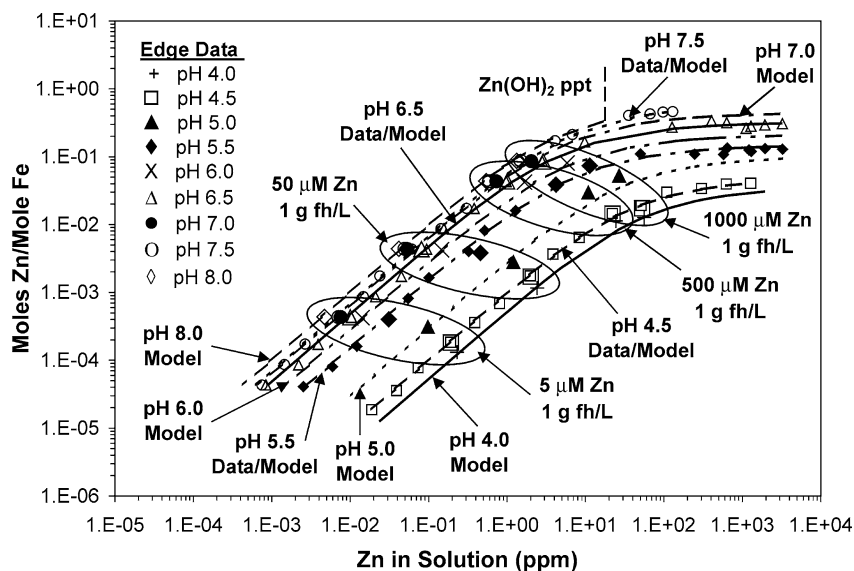


Fig. 2. Comparison of equilibrium isotherm and pH edge data for single-solute Zn(II) sorption onto two-line ferrihydrite to modified triple-layer model predictions using the bidentate-mononuclear surface complex, $(\equiv FeO)_2Zn$. $\log K_{(\equiv FeO)_2Zn}$ and $N_{s,Zn}$ values as f(pH) are given in Table 4. Experimental conditions: 0.1 and 1.0 g of ferrihydrite/l; 0.01 M NaNO₃ background electrolyte for isotherms and edges; Zn(II) added as Zn(NO₃)₂; 4-h equilibration time; room temperature; N₂ glovebox.

ically, a compression in spacing between the constant-pH isotherms at the pH extremes should be expected based on the inherent shape of a pH sorption edge; that is, $d[pZn_{aq}]/d[pH]$ is anything but constant over the path of a pH sorption edge. As shown also for Pb(II) [2], the change in Zn(II) sorbed and, hence, in total Zn_{aq} is fairly small for each one-pH-unit change (i.e., the value of $d[pZn_{aq}]/d[pH]$ is small) at both high and low values of % Zn(II) sorbed. On the other hand, the steep portion of the pH sorption edge is indicative of a much more substantial change in Zn(II) sorbed with pH; that is, $d[pZn_{aq}]/d[pH]$ is large over a fairly narrow pH range. For the case of Zn(II), the steep increase in sorption happens between pH 4.5 and 5.5, where $d[pZn_{aq}]/d[pH]$ peaks at approximately 1.3. As the sorption edge begins to plateau at pH 6, however, $d[pZn_{aq}]/d[pH]$ drops to 0.5 or less.

Figure 3 compares TLM predictions for the bidentate-mononuclear Zn(II) surface complex to pH edge data presented in Trivedi et al. [21]. Figure 3a displays model predictions for 50 μM Zn(II), 1 g of ferrihydrite/l, and 0.001, 0.01, and 0.1 M NaNO_3 using (i) the best-fit equilibrium constant and Zn-active site density for the pH 5.5 isotherm data only and (ii) aqueous activity coefficient corrections for bulk solution ions only (i.e., the ratio of the surface activity coefficients is assumed to equal 1.0) [25]. Note that the model significantly underpredicts Zn(II) sorption at $\text{pH} < 5.0$. Although not obvious in the figure, the model also overpredicts Zn(II) sorption at $\text{pH} \geq 6$. The shallower than expected slope in the pH edge data at low pH was also seen with Pb(II), as previously reported and discussed in detail in Dyer et al. [2]. Others have also reported pH edges for divalent metal sorption onto amorphous ferric hydroxides with this same phenomenon [6,7,10,15,29,30].

In addition, the model curves in Fig. 3a indicate a more significant ionic-strength effect on sorption than do the experimental data. This is most probably an artifact of the thermodynamic framework for the modified TLM itself. As shown also for Pb(II) [2], the mass law expressions utilize bulk solution concentrations and activity coefficients for the sorbing ions (i.e., H^+ , NO_3^- , Na^+ , and Zn^{2+}), rather than the actual surface activities themselves [28]. In addition, because a predictive model does not currently exist for estimating surface activity coefficients, the ratio of the activity coefficients for the surface species (i.e., $(\equiv\text{FeO})_2\text{Zn}$ and $\equiv\text{FeOH}$) is assumed to be 1.0. One might view this as only a “partial correction” for nonidealities at the surface. A surface activity coefficient term (γ_s) was introduced to the model, therefore, to adjust for this overdependence on ionic strength within the OLI thermodynamic framework. Good agreement between the experimental data and the model was achieved when γ_s was set equal to $\gamma_{\text{Zn}^{2+}}$ (the bulk solution activity coefficient for the Zn^{2+} ion). The model curves in Figs. 1 and 2, as well as the equilibrium constants given in Table 4, are based on the use of this surface activity coefficient term.

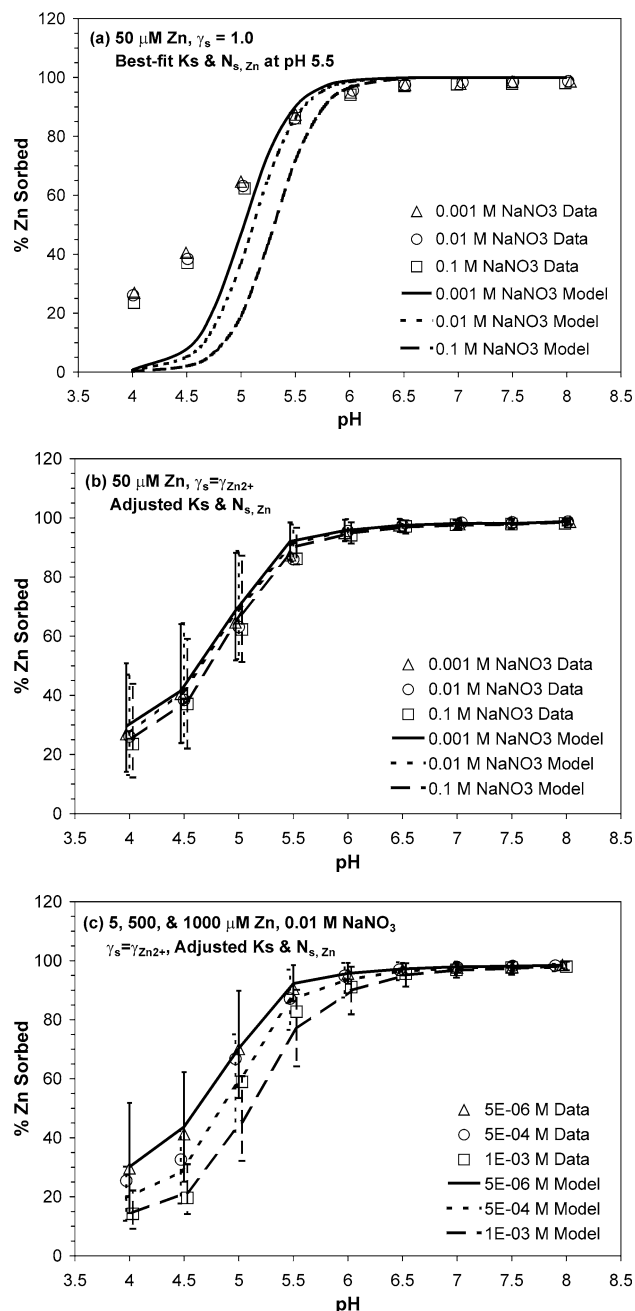


Fig. 3. Triple-layer model predictions of pH sorption edge data for single-solute Zn(II) sorption onto two-line ferrihydrite using the bidentate-mononuclear surface complex, $(\equiv\text{FeO})_2\text{Zn}$. Plots for (a) 50 μM Zn(II) in 0.001–0.1 M NaNO_3 using the best-fit K value and $N_{s,\text{Zn}}$ for pH 5.5 isotherm data only and assuming $\gamma_s = 1.0$; (b) 50 μM Zn(II) in 0.001–0.1 M NaNO_3 using pH-adjusted K values and $N_{s,\text{Zn}}$ values from Table 4 and $\gamma_s = \gamma_{\text{Zn}^{2+}}$ correction; (c) 5, 500, and 1000 μM Zn(II) in 0.01 M NaNO_3 using pH-adjusted K values and $N_{s,\text{Zn}}$ values from Table 4 and $\gamma_s = \gamma_{\text{Zn}^{2+}}$ correction. Ninety-five percent confidence intervals for the model predictions are also shown in (b) and (c). Experimental conditions: 1.0 g of ferrihydrite/l; Zn(II) added as $\text{Zn}(\text{NO}_3)_2$; 4-h equilibration time; room temperature; N_2 glovebox.

Figures 3b and 3c show TLM predictions for the bidentate-mononuclear surface complex when pH-adjusted K values and site densities ($N_{s,\text{Zn}}$) are used in addition to the

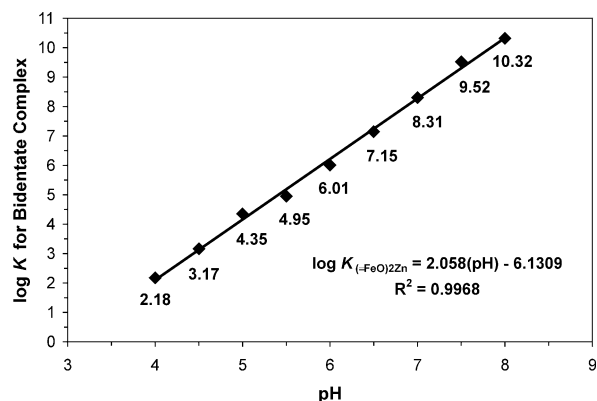


Fig. 4. Linear relationship between $\log K$ (at 1 g of ferrihydrite/l) and pH for the bidentate-mono-nuclear Zn(II) surface complex, $(\equiv\text{FeO})_2\text{Zn}$. Experimental conditions: 1.0 g of ferrihydrite/l; Zn(II) added as $\text{Zn}(\text{NO}_3)_2$; 4-h equilibration time; room temperature; N_2 glovebox.

γ_s correction. More specifically, the $\log K$ value for the bidentate Zn(II) surface complex was $f(\text{pH})$ as shown in Table 4. When this is done, the agreement between the model-predicted curves and the experimental data is good. In contrast to past modeling studies that are based on pH edge data alone, the improved fit at $\text{pH} < 4.5$ was achieved without including additional surface species or a second, high-affinity site for Zn(II). While adding a second, high-affinity sorption site for Zn(II) to the model could account for the elevated Zn(II) sorption at $\text{pH} < 4.5$, it led to poor fits of the isotherm data at dilute Zn(II) concentrations. When considered together, however, the constant-pH isotherm and pH sorption edge data suggest that a one-Zn-sorption-site, one-species model is adequate, which is also consistent with the spectroscopic findings [21].

A downside of this investigation is that the best-fit equilibrium constants and site densities appear to be functions of pH as the TLM is currently constructed. Interestingly, Fig. 4 shows that there is a linear relationship between $\log K_{(\equiv\text{FeO})_2\text{Zn}}$ and pH. The same was found to be true for model regressions using the surface complex, $\equiv\text{FeOZnOH}$ (figure not shown; see Dyer [23]). The reason for this linear relationship is not clear at the present time; however, it does provide a useful correlation to estimate the conditional equilibrium constant for the bidentate-mono-nuclear complex.

3.3. Uncertainty in isotherm and pH edge data

Uncertainty bars (95% confidence intervals) for the constant-pH-isotherm model predictions are shown in Fig. 1b. Uncertainty bars are not shown for every data point for clarity. The experimental data points fall comfortably within the uncertainty bars in all cases. As shown in the figure, the uncertainty ranges for Zn_{aq} tend to be much wider than those for Zn_{sorb} , especially at $\text{pH} 5.5$ and above.

For select isotherm data points, Tables 5 and 6 show the fractions of the total output uncertainty in Zn_{aq} and Zn_{sorb} , respectively, that is attributable to specific input/thermodynamic parameters. The values in the tables for each input/

Table 5
Input/thermodynamic parameters dominating output uncertainty in Zn_{aq} (ppm) for the Zn(II)/ferrihydrite constant-pH isotherms shown in Fig. 1b (1 g of ferrihydrite/l except where noted)

pH	Zn total (M)	Fraction of output COV squared for Zn_{aq}					
		Total	Total	Total	pH	$\log K_{(\equiv\text{FeO})_2\text{Zn}}^{\text{int}}$	$\log K_{\text{NO}_3^-}^{\text{int}}$
		H ₂ O	Zn	ferrihydrite			
4.5	2E-02	0.68	0.32	–	–	–	–
	1E-03	0.13	0.13	0.31	0.06	0.30	0.07
	2E-04	–	0.03	0.26	0.09	0.51	0.11
	2E-06	–	0.01	0.22	0.11	0.55	0.11
5.5	2E-02	0.62	0.33	0.05	–	–	–
	1E-03	–	0.02	0.50	0.07	0.38	0.03
	2E-04	–	–	0.28	0.11	0.57	0.03
	2E-06	–	–	0.24	0.12	0.61	0.03
6.5	2E-02	0.46	0.30	0.23	–	–	–
	1E-03	–	–	0.37	0.10	0.52	–
	2E-04	–	–	0.26	0.12	0.61	–
	2E-06	–	–	0.24	0.12	0.63	–
7.5 (0.1 g/l)	2E-03	0.25	0.22	0.45	–	0.08	–
	1E-03	–	–	0.31	0.11	0.58	–
	2E-04	–	–	0.26	0.11	0.62	–
	2E-06	–	–	0.25	0.11	0.63	–

thermodynamic parameter represent the fraction of the output COV squared [23]. As shown in Table 5, at Zn(II) surface loadings lower than those approaching site saturation, uncertainties in $\log K_{(\equiv\text{FeO})_2\text{Zn}}^{\text{int}}$ and, to a lesser degree, total ferrihydrite dominate the output uncertainty in Zn_{aq} for all pH. As surface loading increases, the relative importance of total ferrihydrite increases relative to $\log K_{(\equiv\text{FeO})_2\text{Zn}}^{\text{int}}$. On the other hand, as site saturation is approached, uncertainties in total H₂O, total Zn, and, at higher pH, total ferrihydrite dominate the uncertainty in Zn_{aq} . For sorbed Zn, Table 6 shows that the uncertainty in total ferrihydrite dominates the output uncertainty in Zn_{sorb} at pH 5.5 and above, except near site saturation where $\log K_{(\equiv\text{FeO})_2\text{Zn}}^{\text{int}}$ and, to a lesser extent, pH dominate the output uncertainty. At pH 4.5, on the other hand, uncertainties in $\log K_{(\equiv\text{FeO})_2\text{Zn}}^{\text{int}}$ and, to a lesser extent, $\log K_{\text{NO}_3^-}^{\text{int}}$ and pH dominate the uncertainty in Zn_{sorb} . Input/thermodynamic parameters listed in Table 2, but not shown in Tables 5 and 6, had a negligible impact on the output uncertainty under all conditions.

Figs. 3b, 3c display the uncertainty bars (95% confidence intervals) for six TLM-predicted pH sorption edges for single-solute Zn(II) sorption onto ferrihydrite. Once again, the experimental data fall well within the uncertainty bars for the model predictions. Note the large uncertainty in percent Zn sorbed over most of the pH range of the edges. This reinforces the point that regression of pH sorption edge data alone is not a sufficient test of the predictive capability of a SCM. Regression of constant-pH isotherm data at multiple pH values, together with pH edge data at several ionic strengths and metal/sorbent molar ratios, is a necessary approach.

Table 6

Input/thermodynamic parameters dominating output uncertainty in Zn_{sorb} (mol Zn/mol Fe) for the Zn(II)/ferrihydrite constant-pH isotherms shown in Fig. 1b (1 g of ferrihydrite/l except where noted)

pH	Zn total (M)	Fraction of output COV squared for Zn_{sorb}					
		Total	Total	Total	pH	$\log K_{(\equiv FeO)_2 Zn}^{int}$	$\log K_{NO_3^-}^{int}$
		H ₂ O	Zn	ferrihydrite			
4.5	2E-02	0.02	–	0.06	0.11	0.59	0.22
	1E-03	0.02	–	0.03	0.13	0.66	0.15
	2E-04	0.02	–	0.01	0.13	0.68	0.14
	2E-06	0.02	–	–	0.13	0.69	0.14
5.5	2E-02	0.02	–	0.06	0.13	0.67	0.12
	1E-03	0.02	0.04	0.27	0.10	0.53	0.04
	2E-04	–	0.05	0.79	0.02	0.13	–
	2E-06	–	0.05	0.85	0.02	0.08	–
6.5	2E-02	0.02	–	0.05	0.14	0.74	0.05
	1E-03	–	0.05	0.92	–	0.03	–
	2E-04	–	0.04	0.95	–	0.01	–
	2E-06	–	0.04	0.95	–	–	–
7.5 (0.1 g/l)	2E-03	0.03	–	0.03	0.14	0.79	–
	1E-03	–	0.04	0.95	–	–	–
	2E-04	–	0.04	0.95	–	–	–
	2E-06	–	0.04	0.95	–	–	–

Table 7

Input/thermodynamic parameters dominating output uncertainty in percent Zn sorbed for the Zn(II)/ferrihydrite pH sorption edges shown in Figs. 3b, 3c (1 g of ferrihydrite/l)

pH	Zn total (M)	Fraction of output COV squared for % Zn_{sorb}					
		Total	Total	Total	pH	$\log K_{(\equiv FeO)_2 Zn}^{int}$	$\log K_{NO_3^-}^{int}$
		H ₂ O	Zn	ferrihydrite			
4.0	5E-06	0.02	0.21	0.10	0.10	0.53	0.14
	5E-05	0.02	0.22	0.10	0.10	0.52	0.14
	1E-03	0.01	0.37	0.08	0.08	0.41	0.13
5.0	5E-06	0.02	0.23	0.11	0.11	0.59	0.05
	5E-05	0.02	0.24	0.11	0.11	0.58	0.05
	1E-03	0.01	0.43	0.08	0.08	0.42	0.05
6.0	5E-06	0.02	0.24	0.12	0.12	0.61	0.01
	5E-05	0.02	0.24	0.12	0.12	0.61	0.01
	1E-03	0.01	0.44	0.09	0.09	0.45	0.01
7.0	5E-06	0.02	0.24	0.12	0.12	0.62	–
	5E-05	0.02	0.25	0.12	0.12	0.61	–
	1E-03	0.02	0.33	0.10	0.10	0.55	–
8.0	5E-06	0.02	0.25	0.10	0.10	0.63	–
	5E-05	0.02	0.25	0.10	0.10	0.63	–
	1E-03	0.02	0.31	0.09	0.09	0.58	–

For select pH edge data points, Table 7 shows the fraction of the total output uncertainty in % Zn_{sorb} that is attributable to specific input/thermodynamic parameters. For Zn(II) surface loadings less than those approaching site saturation, uncertainties in $\log K_{(\equiv FeO)_2 Zn}^{int}$ and, to a lesser degree, total ferrihydrite and pH dominate the output uncertainty in % Zn_{sorb} . As surface loading decreases, the importance of $\log K_{(\equiv FeO)_2 Zn}^{int}$ relative to total ferrihydrite

increases for all pH. Conversely, as surface loading increases and pH decreases, the importance of total ferrihydrite relative to $\log K_{(\equiv FeO)_2 Zn}^{int}$ increases. Uncertainties in $\log K_{NO_3^-}^{int}$ are only of secondary importance at pH < 4.5. This trend is similar to what was observed for the constant-pH-isotherm Zn_{aq} data in Table 5. At all pH and Zn(II) surface loadings, the impact of uncertainties in pH on the uncertainty in % Zn_{sorb} is about the same (8–12%). Input/thermodynamic parameters listed in Table 2, but not shown in Table 7, had a negligible impact on the output uncertainty under all conditions.

4. Summary

As was found for single-solute Pb(II) sorption onto ferrihydrite [2], regressing potentiometric titration, pH sorption edge, and constant-pH isotherm data collected over a broad range of conditions is a much more rigorous test of a SCM. When supplemented with spectroscopic analyses to confirm surface speciation, the scope of feasible surface complexes and site types for the model becomes much more limited. In particular, this research highlights the value of coupling surface complexation modeling with an extensive array of molecular- and macroscopic-scale studies performed by the same investigator in the same laboratory. The current results for Zn, along with the previous results for Pb [2], lead to similar conclusions about the ability of the modified TLM to predict trace-metal sorption over a wide range of conditions. First, extensive independent modeling of the Zn(II) and Pb(II) sorption data using the modified TLM strongly supported the conclusions about surface speciation gleaned from the spectroscopy data presented and analyzed in Trivedi et al. [21,22]. Second, regression of pH edge data in the absence of isotherm and spectroscopic data results in a much larger number of surface species and site type combinations that provide acceptable fits of the edge data. However, when these same assumptions are used to predict the constant-pH isotherms, the agreement between model and data is poor in most cases. Third, a unique set of surface complexation equilibrium constants and corresponding site densities is unable to describe Zn(II) and Pb(II) sorption onto ferrihydrite. In both cases, the regressed equilibrium constants for the Pb(II) and Zn(II) surface complexes were functions of pH; therefore, they must be viewed as conditional equilibrium constants, rather than true intrinsic equilibrium constants. For Zn(II), the density of Zn sorption sites was also found to vary with pH.

In conclusion, the results of this research and previous work with Pb(II) indicate that the existing thermodynamic framework for the modified TLM is able to reproduce the metal sorption data only over a limited range of pH, concentration, and ionic strength conditions. For this reason, much work still needs to be done in fine-tuning the thermodynamic framework and databases for the TLM.

Acknowledgments

This research was supported by funding from the DuPont Company and the State of Delaware through the Delaware Research Partnership. The authors particularly thank Drs. Jehangir Vevai and Hugh Campbell for their financial support and Mr. Steve Sanders and Dr. Marshall Rafal (OLI Systems Inc.) for their important contributions to the implementation of surface complexation models in the OLI Software. We are also grateful to two anonymous reviewers for their comments.

Appendix A

a_i	activity of species i
A_s	specific surface area of sorbent (m^2/g)
C_1	inner-layer capacitance term for triple-layer model ($\text{faraday}/\text{m}^2$)
C_2	outer-layer capacitance term for triple-layer model ($\text{faraday}/\text{m}^2$)
COV_i	coefficient of variation (σ_{Y_i}/Y_i)
F	Faraday's constant ($96,485 \text{ C/mol}$)
K_i	conditional equilibrium constant
K_i^{int}	intrinsic or thermodynamic equilibrium constant
K_{a1}^{int}	intrinsic acidity constant for the surface deprotonation reaction: $\equiv\text{FeOH}_2^+ \rightleftharpoons \equiv\text{FeOH} + \text{H}^+$
K_{a2}^{int}	intrinsic acidity constant for the surface deprotonation reaction: $\equiv\text{FeOH} \rightleftharpoons \equiv\text{FeO}^- + \text{H}^+$
$N_{s, \text{total}}$	proton-active site density (mol of sites/mol of sorbent)
$N_{s, \text{Zn}}$	Zn-active site density (mol of sites/mol of sorbent)
R	gas constant ($8.314 \text{ J mol}^{-1} \text{ K}^{-1}$)
R_{avg}	arithmetic average of nonlinear regression fit parameters obtained from the OLI Software (R_i for each data point is the ratio of the model-calculated value to the experimental value (or vice versa), such that R_i is 1.0 or higher)
T	absolute temperature (K)
Zn_{aq}	total zinc(II) in bulk aqueous solution (mg l^{-1} or mol/kg of H_2O)
Zn_{sorb}	total zinc(II) sorbed on surface of ferrihydrite (mol of Zn(II)/mol of Fe)
$\Delta \text{p}K_a$	equals ($\text{p}K_{a2}^{\text{int}} - \text{p}K_{a1}^{\text{int}}$) when the protonation/deprotonation reactions are written as dissociation reactions
γ_s	lumped surface activity coefficient used in OLI model to account for nonidealities of the surface complex species
Γ	surface loading (mol of Zn(II)/mol of Fe)
Ψ_0	electric potential at 0-plane
Ψ_β	electric potential at β -plane
σ_i	standard deviation of variable i

References

- [1] D.A. Dzombak, F.M.M. Morel, Surface Complexation Modeling: Hydrous Ferric Oxide, Wiley, New York, 1990.
- [2] J.A. Dyer, P. Trivedi, N.C. Scrivner, D.L. Sparks, Environ. Sci. Technol. 37 (2003) 915–922.
- [3] D.G. Kinniburgh, M.L. Jackson, J.K. Syers, Soil Sci. Soc. Am. J. 40 (1976) 796–799.
- [4] R.R. Gadde, H.A. Laitinen, Anal. Chem. 46 (1974) 2022–2026.
- [5] J.O. Leckie, M.M. Benjamin, K.F. Hayes, G. Kaufman, S. Altmann, Adsorption/Coprecipitation of Trace Elements from Water with Iron Oxyhydroxide, CS-1513, Electric Power Research Institute, Palo Alto, CA, 1980.
- [6] M.M. Benjamin, N.S. Bloom, in: P.H. Tewari (Ed.), Adsorption from Aqueous Solutions, Plenum, New York, 1981, pp. 41–60.
- [7] M.M. Benjamin, Environ. Sci. Technol. 17 (1983) 686–692.
- [8] M.F. Schultz, M.M. Benjamin, J.F. Ferguson, Environ. Sci. Technol. 21 (1987) 863–869.
- [9] R.J. Crawford, I.H. Harding, D.E. Mainwaring, Langmuir 9 (1993) 3050–3056.
- [10] N.Z. Misak, H.F. Ghoneimy, T.N. Morcos, J. Colloid Interface Sci. 184 (1996) 31–43.
- [11] D.G. Kinniburgh, K. Sridhar, M.L. Jackson, in: Proceedings of the 15th Hanford Life Sciences Symposium on Biological Implications of Metals in the Environment, USERDA-NTIS, Hanford, WA, 1977, pp. 231–239.
- [12] M.M. Benjamin, Effects of Competing Metals and Complexing Ligands on Trace Metal Adsorption at the Oxide/Solution Interface, Ph.D. dissertation, Stanford University, Stanford, CA, 1979.
- [13] B.A. Dempsey, P.C. Singer, in: R.A. Baker (Ed.), Contaminants and Sediments, Vol. 2, Analysis, Chemistry, and Biology, Ann Arbor Science, Ann Arbor, 1980, pp. 333–352.
- [14] D.G. Kinniburgh, M.L. Jackson, Soil Sci. Soc. Am. J. 46 (1982) 56–61.
- [15] D.T. Harvey, R.W. Linton, Colloids Surf. 11 (1984) 81–96.
- [16] S.B. Kanungo, J. Colloid Interface Sci. 162 (1994) 93–102.
- [17] P. Trivedi, L. Axe, Environ. Sci. Technol. 34 (2000) 2215–2223.
- [18] K.F. Hayes, Equilibrium, Spectroscopic, and Kinetic Studies of Ion Adsorption at the Oxide/Aqueous Interface, Ph.D. Dissertation, Stanford University, Stanford, CA, 1987.
- [19] G.E. Brown Jr., G.A. Parks, J.R. Bargar, S.N. Towle, in: D.L. Sparks, T.J. Grundl (Eds.), Mineral–Water Interfacial Reactions: Kinetics and Mechanisms, in: ACS Symposium Series, Vol. 715, American Chemical Society, Washington, DC, 1998, pp. 14–36.
- [20] L.E. Katz, E.J. Boyle-Wight, in: H.M. Selim, D.L. Sparks (Eds.), Physical and Chemical Processes of Water and Solute Transport/Retention in Soil, SSSA Special Publication No. 56, Soil Science Society of America, Madison, WI, 2001, pp. 213–255.
- [21] P. Trivedi, J.A. Dyer, D.L. Sparks, J. Colloid Interface Sci. in press.
- [22] P. Trivedi, J.A. Dyer, D.L. Sparks, Environ. Sci. Technol. 37 (2003) 908–914.
- [23] J.A. Dyer, Advanced Approaches for Modeling Trace Metal Sorption in Aqueous Systems, Ph.D. dissertation, University of Delaware Newark, DE, 2002.
- [24] S.J. Sanders, M. Rafal, D.M. Clark, R.D. Young, N.C. Scrivner, R.A. Pease, S.L. Grise, R.B. Diemer, Chem. Eng. Prog. 92 (1988) 47–54.
- [25] N. Sahai, D.A. Sverjensky, Comput. Geosci. 24 (1998) 853–873.
- [26] K.F. Hayes, L.E. Katz, in: P.V. Brady (Ed.), Physics and Chemistry of Mineral Surfaces, CRC Press, Boca Raton, FL, 1996, pp. 147–223.
- [27] D.L. Sparks, Environmental Soil Chemistry, Academic Press, San Diego, 1995.
- [28] A.P. Robertson, J.O. Leckie, J. Colloid Interface Sci. 188 (1997) 444–472.
- [29] J.A. Davis, J.O. Leckie, J. Colloid Interface Sci. 67 (1978) 90–107.
- [30] K.C. Swallow, D.N. Hume, F.M.M. Morel, Environ. Sci. Technol. 14 (1980) 1326–1331.